International Journal of Coal Science & Technology (2023) 10:72
https://doi.org/10.1007/s40789-023-00655-9

RESEARCH

Effect of CO_2 dilution on laminar burning velocities, combustion characteristics and NO_x emissions of CH_4/air mixtures

Wenlong Dong[1] · Longkai Xiang[2] · Jian Gao[1] · Bingbing Qiu[1] · Huaqiang Chu[1]

Received: 2 February 2023 / Revised: 14 September 2023 / Accepted: 23 October 2023

Abstract

The laminar combustion characteristics of CH_4/air premixed flames with CO_2 addition are systemically studied. Experimental measurements and numerical simulations of the laminar burning velocity (LBV) are performed in CH_4/CO_2/Air flames with various CO_2 doping ratio under equivalence ratios of 1.0–1.4. GRI 3.0 mech and Aramco mech are employed for predicting LBV, adiabatic flame temperature (AFT), important intermediate radicals (CH_3, H, OH, O) and NO_x emissions (NO, NO_2, N_2O), as well as the sensitivity analysis is also conducted. The detail analysis of experiment and simulation reveals that as the CO_2 addition increases from 0% to 40%, the LBVs and AFTs decrease monotonously. Under the same CO_2 doping ratio, the LBVs and AFTs increase first and then decrease with the increase of equivalence ratio, and the maximum of LBV is reached at equivalence ratio of 1.05. The mole fraction tendency of important intermediates and NO_x with equivalence ratio and CO_2 doping ratio are similar to the LBVs and AFTs. Reaction $H + O_2 \Leftrightarrow O + OH$ is found to be responsible for the promotion of the generation of important intermediates and NO_x under the equivalence ratios and CO_2 addition through sensitivity analysis. The sensitivity coefficients of elementary reactions that the increasing of CO_2 doping ratio promotes or inhibits formation of intermediate radicals and NO_x decreases.

✉ Huaqiang Chu
hqchust@163.com

Bingbing Qiu
bingbingq@126.com

[1] School of Energy and Environment, Anhui University of Technology, Ma'anshan 243002, People's Republic of China

[2] Key Laboratory for Power Machinery and Engineering of Ministry of Education (MOE), Shanghai Jiao Tong University, Shanghai 200240, People's Republic of China

Published online: 13 November 2023

Graphical abstract

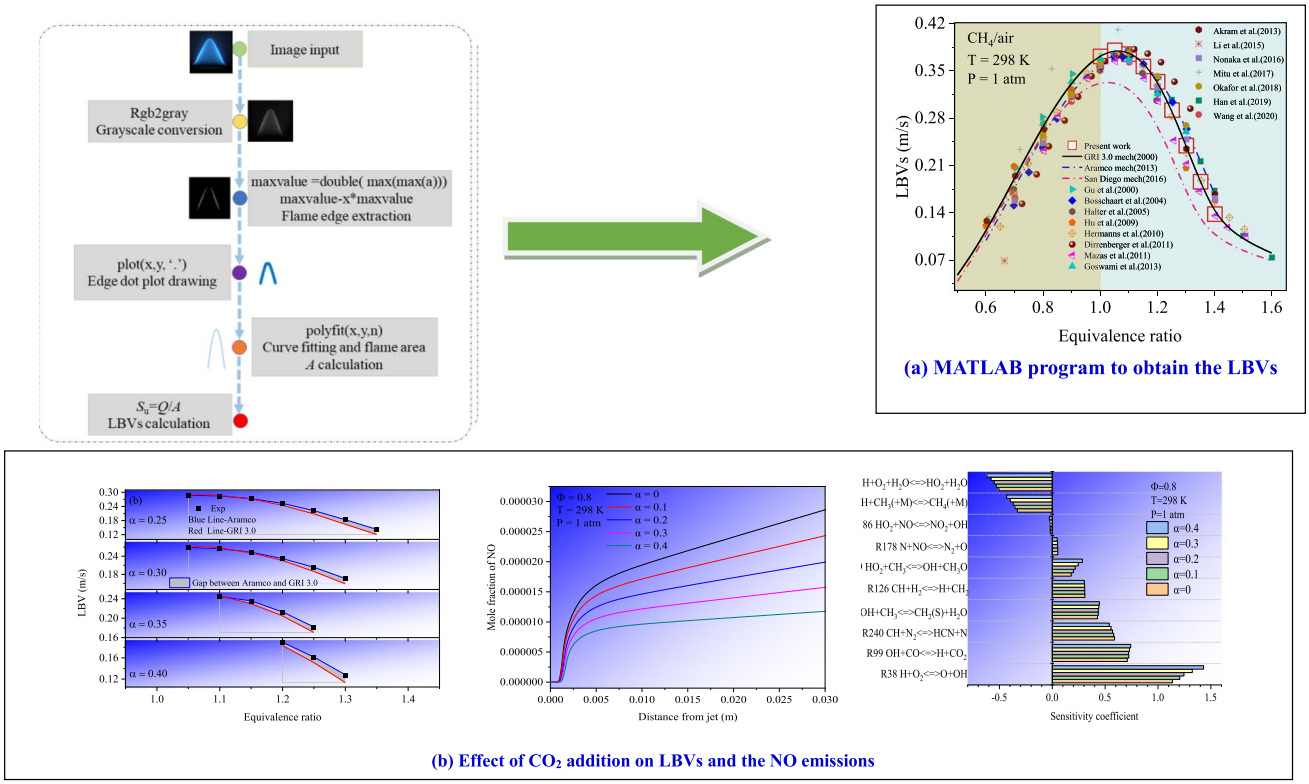

Keywords CO_2 dilution · Laminar burning velocity · Adiabatic flame temperature · Sensitivity analysis

List of symbols

AFT	Adiabatic flame temperature
CH_4	Methane
CO_2	Carbon dioxide
LBV	Laminar burning velocity
MFC	Mass flow controller
N_2	Nitrogen
O_2	Oxygen
$V_{diluent}$	Volume fractions of dilution gas
V_{fuel}	Volume fractions of dilution fuel
Φ	Equivalence ratio
α	CO_2 doping ratio
$\dot{m}_{fuel}$	Mass flow rates of fuel
$\dot{m}_{air}$	Mass flow rates of oxidant

1 Introduction

Carbon dioxide (CO_2) and methane are responsible for global warming and climate change. Human beings must solve a series of problems related to global warming, and greenhouse gas emissions is the main factor leading to this problem (Wang et al. 2021; Li and Fang 2014). In order to cope with the high CO_2 concentration in the atmosphere, it is necessary to reduce carbon emissions through various methods. CO_2 capture and utilization have attracted more and more attention, such as CO_2 capture (Talapaneni et al. 2019; Huang et al. 2019) and conversion of CO_2 to hydrocarbons (Ao et al. 2020; Guo et al. 2019; Zhang et al. 2021; Shamiri et al. 2016). Besides, exploring the effect of CO_2 dilution on the fuel combustion (e.g., hydrocarbons, synthesis gas, biogas, etc.) is also one of the important research fields. Exhaust gas recirculation (EGR) has been shown to be an effective method to reduce NO_x emissions and improve burst resistance. EGR contains gases consisting a large amount of CO_2, and EGR affects the combustion process through three pathways: (1) thermal, (2) dilution, and (3) chemical effects (Wang et al. 2022). CO_2 is also required as a diluent for both moderate and intense low oxygen dilution combustion and oxyfuel combustion (Liu et al. 2020). Methane, as the simplest hydrocarbon fuel, is of great theoretical and practical importance for the study of its blending and combustion with CO_2. Laminar combustion is the basis of turbulent combustion and the cornerstone of further study of combustion and it can reflect various combustion characteristic parameters such as laminar burning velocity, ignition energy, maximum

flame temperature, ignition delay, ignition temperature and concentration of fuel (Movileanu et al. 2011). Laminar burning velocity (LBV) is an inherent characteristic of fuel and an important parameter for laminar flame propagation and stability. Laminar burning velocity depends on the type and composition of fuel and initial conditions such as equivalence ratio, pressure and temperature, and contains important information such as reaction, diffusion, heat release, tempering, instability, etc. (Chu et al. 2020; Nonaka and Pereira 2016; Zhang et al. 2015). It's a very vital parameter in the design effective control of combustion systems, such as the design and manufacture of combustors and explosion suppression devices, and the optimization of internal combustion engines (Hu et al. 2009a, b; Dirrenberger et al. 2011; Razus et al. 2010; Ren et al. 2019a, b; Chu et al. 2019).

Sampath et al. (2023) investigated the effect of CO_2 on the laminar burning velocity of CH_4/air at high temperatures by using the externally heated diverging channel (EHDC) method. It was shown that the dilution of CO_2 enhances the competition for H-atom consumption, and the LBV increased with the increase of the mixture and decreased with the proportion of doped CO_2. Ghabi et al. (2023) studied the effect of microsecond pulsed plasma on non-premixed biogas. Shang et al. (2022) systematically investigated the effect of N_2/CO_2 on H_2/CH_4/air laminar flame velocity. Ueda et al. (2021) explored the effect of CO_2 on the premixed combustion characteristics of methane/air using the spherical expansion method. Jithin et al. (2020) investigated the combined effect of CO_2/N_2 dilution on the laminar combustion rate of methane/oxygen by heat flux method and numerical simulation. The results showed that the laminar burning velocity decreased with increasing proportion of blended CO_2 and it is found that the laminar burning velocity decreased more in the fuel-rich combustion case than in the fuel-lean combustion and stoichiometric ratio. Anggono et al. (2020) investigated the effect of CO_2 concentration on the laminar burning velocity and Markstein length of CH_4/air premixed flames at high pressure constant volume combustion. It was shown that there is a monotonic relationship between the Markstein length and the CO_2 dilution ratio and that the unstretched laminar burning velocity of the mixture decreased with increasing CO_2 concentration. Azatyan et al. (2010) reported the effect of CH_4, N_2, CO_2 and steam addition on the LBVs of H_2. The predictions showed that with the increase of H_2 doping ratio, the LBVs of H_2/Air monotonically decreased, but did not exceed 1.5 times, and the AFTs changed slowly. The effect of CO_2 and N_2 on the flame stability and LBVs of syngas/air was successfully performed by Burbano et al. (2011). Through experimental and numerical simulations, Burbano et al. (2011) showed that with the increase of CO_2 dilution doping ratio, the LBVs decreased obviously due to the decrease of heat release and the increase of heat capacity. This conclusion was consistent with the conclusion of Ref. Wang et al. (2012) measured the LBVs of $CO/H_2/CO_2/O_2$ by using spherical flame. The experimental results proved that H_2 and CO_2 have opposite effects on the LBV of syngas. Sun and Xu (2020) conducted the relationship between turbulent burning velocity and H_2 content in synthesis gas and revealed that turbulent burning velocity was a second-order polynomial of hydrogen volume fraction. Based on heat flux method and Bunsen burner, Wang et al. (2015) measured the LBVs of $CO/H_2/N_2/CO_2$ and numerically analyzed the effect of H and OH radicals on the LBV of syngas. The results showed that H had a linear relationship with LBVs. Nonaka and Pereira (2016) studied the effect of CO_2 addition in biogas on LBVs. The LBVs and other combustion characteristics of the natural gas blended with N_2, CO_2 and H_2O were carried out by Ren et al. (2019a, b, 2020). In addition, the effects of CO_2 on NO_x formation of methane combustion products were also conducted. Xiang et al. (2019, 2020) numerically investigated the chemical and physical effects of CO_2 and H_2 on LBVs and other laminar combustion characteristics of CH_4.

In view of the above considerations, the first objective is to investigate the effect of blending a wide range of CO_2 concentrations on methane combustion characteristics through a combination of experimental and numerical simulations. The second objective is to analyze the effect of CO_2 on NO_x generation during methane combustion, from the molar amount of NO_x to the temperature sensitivity of NO_x. There have been many studies on the effect of CO_2 on methane combustion characteristics, but few have addressed the effect of CO_2 blending into methane in terms of temperature sensitivity and NO_x generation. Therefore, this work conducts a study on the laminar combustion characteristics and NO_x emission of methane blended with CO_2.

2 Experiment setup

The laminar premixed flame experimental system is shown in Fig. 1. The experimental systems were mainly divided into: Bunsen burner, gas delivery system, gas supply system and safety system. The Bunsen burner mainly consists of a lamp body section and a lamp nozzle connected. The inner cavity of the lamp body section is equipped with a packing layer, a flow equalizing plate and a sintered net from bottom to top. The device plays a role in stabilizing the flow of the gas mixture flowing through it, and the flame ignited from the lamp nozzle is close to being conical, so that the detection accuracy of the flame propagation speed can be improved. The gas delivery system is completed by mass flow controller (MFC) and mixing tank. The brand of MFC is Sevenstar Huachuang CS200 series with an accuracy of 0.35% of full scale. The gas supply system contains N_2, CO_2, O_2 and CH_4 and the purity of

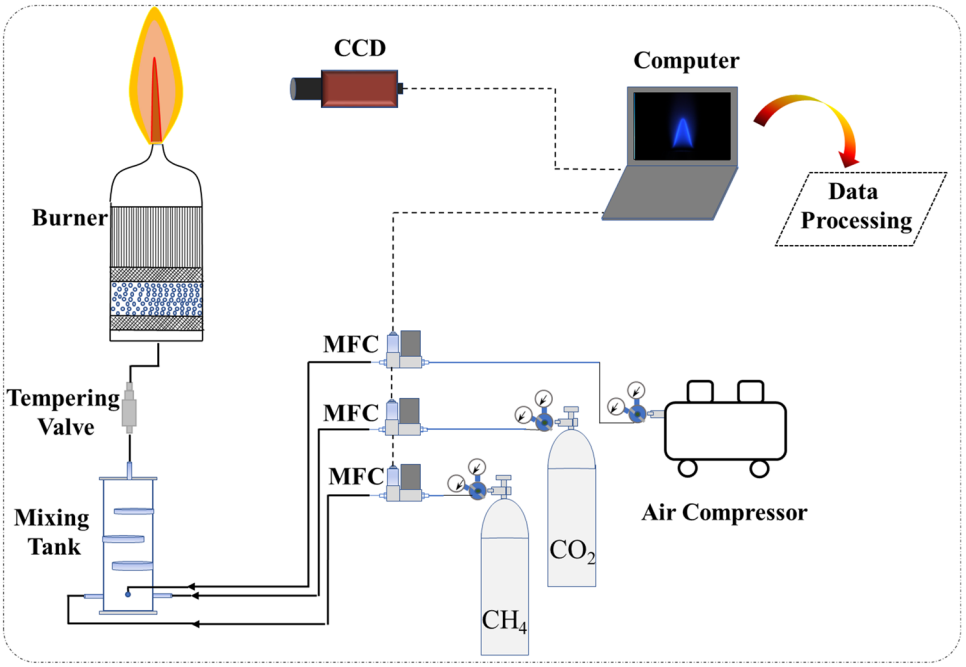

Fig. 1 Experimental apparatus for the combustion of CH_4/air mixtures with diluted CO_2

CH_4, N_2, CO_2 and O_2 are 99.99%. The safety system is tempering valve, which is to prevent the flame from flowing back to the mixing tank to explode. After the gas through the flowmeter and mixing tank, it passes the channel at the bottom of the burner, glass beads, flow equalization plates and multi-layer metal sintering net to form a stable conical flame at the nozzle. Besides, an industrial camera is used to photograph the flame image. The flame images are obtained by a CCD camera, model MANTA G-504C manufactured in Germany. The CCD camera chip is the Sony ICX655, the response frequency range is visible light. The image acquisition is realized by connecting the CCD camera port with the computer port through a Gigabit Ethernet cable. This model of CCD camera can be very good completion of the experimental process in the acquisition of flame images.

2.1 CO_2 doping ratio

$CH_4/CO_2/N_2/O_2$ is studied under premixed combustion at 298 K and 1 atm. The sum of CH_4 and dilution is 1, that is, the content of methane in mixtures decreases with increasing dilution gas content. Therefore, the general formula for calculating the doping ratio is:

$$\alpha = \frac{V_{\text{diluent}}}{V_{\text{diluent}} + V_{\text{fuels}}} \tag{1}$$

where V_{diluent} and V_{fuels} are volume fractions of dilution gas and fuel, respectively. α represents the proportion of dilution gas in the mixture.

Therefore, in the mixture, α is defined as the CO_2 doping ratio, and the formula is as follow:

$$\alpha = \frac{V_{CO_2}}{V_{CO_2} + V_{CH_4}} \tag{2}$$

where V_{CO_2} is the volume fraction of CO_2. V_{CH_4} denotes the volume fraction of methane in the mixture. In this paper, $CH_4/O_2/N_2$ mixed with CO_2 content of 0%–40% ($\alpha = 0$, 5%, 10%, 15%, 20%, 25%, 30%, 35%, 40%) is systematically analyzed.

The effect of CO_2 on the laminar combustion of methane is different, because of the different properties of CO_2 and N_2. During the experiment of mixing carbon dioxide with methane, we found that when the flow rates of methane were set at 280 mL/min and 260 mL/min, more experiments could be carried out. Therefore, in the experiments of mixing methane with carbon dioxide, the flow rates of methane are 280 mL/min and 260 mL/min. Table S1 in Supplementary information presents the experimental operation of CH_4/Air/CO_2 flame.

2.2 Laminar burning velocity calculation

Figure 2 shows the images obtained by CCD camera. The work conditions of $\Phi = 1.2$ are selected to show the images of methane mixed with carbon dioxide with doping ratios.

After capturing the images of premixed flame, the MATLAB code is used to calculate the LBVs of mixtures. The main steps to obtain the LBVs of CH_4 can be found in Ref

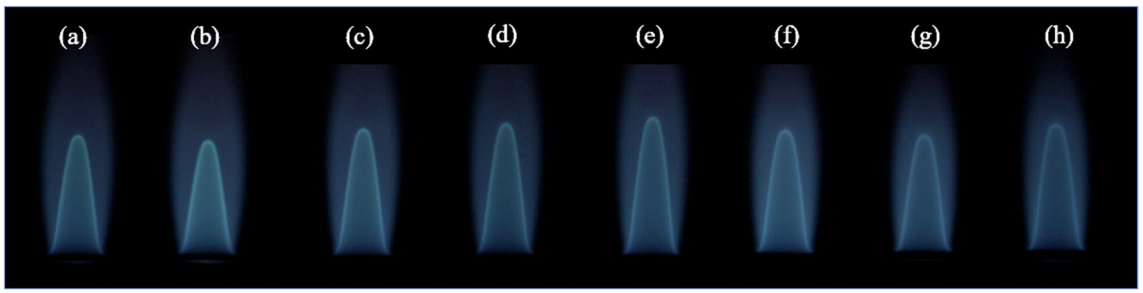

Fig. 2 Images obtained from CCD camera under methane/air with different CO_2 doping ratios. **a** $\alpha=5\%$. **b** $\alpha=10\%$. **c** $\alpha=15\%$. **d** $\alpha=20\%$. **e** $\alpha=25\%$. **f** $\alpha=30\%$. **g** $\alpha=35\%$. **h** $\alpha=40\%$

(Chu et al. 2021). Figure 3 gives the main steps to obtain the LBVs of CH_4 through the MATLAB code.

2.3 Error analysis

In the process of measuring the LBVs with the Bunsen burner, the measurement error is mainly caused by the error of the total gas flow rate (δ_Q) and the error generated when calculating the flame area (δ_A). The error of the total flow of the premixed gas is determined by the error of methane flow rate (δ_{CH_4}), and the accuracy of the methane flowmeter is ± 2% of the upset point, the error of the air flowmeter (δ_{air}), and the error of CO_2 flowmeter (δ_{CO_2}). The accuracy is ± 1% of the set point. According to the error transfer principle, the error calculation method in Refs (Chu et al. 2021; Moffat 1988) can be used to calculate the total gas flow error:

$$\delta_Q=\sqrt{\delta_{CH_4}^2+\delta_{air}^2+\delta_{CO_2}^2}=\sqrt{2^2+1^2+1^2}=\sqrt{6} \quad (3)$$

The error of flame area is mainly determined by the resolution of the camera and the method of experimental photo processing. By calculating the adjacent points of the

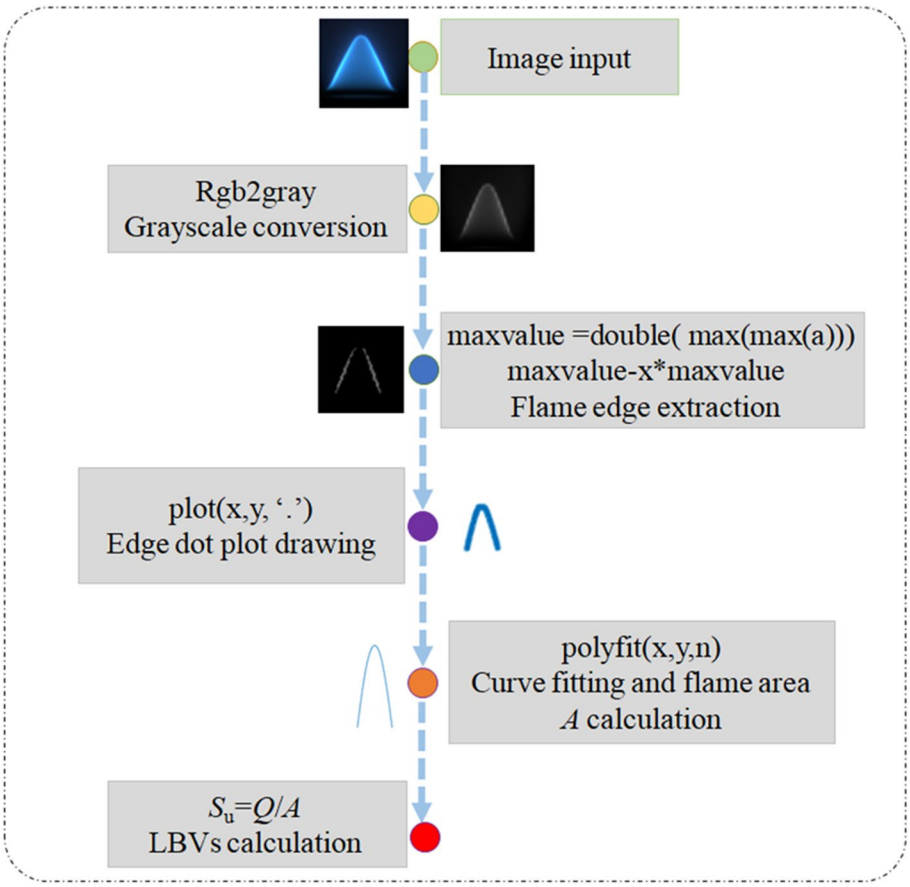

Fig. 3 The major steps of calculating laminar burning velocity by MATLAB code

maximum gradient point in the inner boundary of the flame, the error is 4.5% approximately.

The total calculation error of LBV is:

$$\delta_L = \sqrt{\delta_Q^2 + \delta_A^2} = \sqrt{(\sqrt{6})^2 + (4.5)^2} \approx 5.1\% \quad (4)$$

The calculation error of laminar burning velocity is approximately 5.1% by calculating.

2.4 Modeling details

In the simulation, we choose the CHEMKIN-Pro/PREMIXED code to simulate the effect of CO_2 on methane laminar combustion. Two different reaction mechanisms are used for the calculations, the Aramco mech (Metcalfe et al. 2013) and the GRI 3.0 mech (Simith et al. 2000) and these mechanisms are widely used for the calculations of small molecule hydrocarbon fuels. The Armaco mech contains 493 species and 2716 reactions and the GRI 3.0 mech contains 53 species and 325 reactions. Since the Aramco model does not include the NO_x component, the GRI 3.0 model is used to analyze the effect of CO_2 dilution on NO_x formation. The chemical reactions, thermal properties and transport properties database are imported using CHEMKIN format. The maximum grid number is set to 500, and the parameters chosen for this study ensured grid independence. GRAD and CURV are set to 0.04, and the iteration interval are −0.002 to 0.06 m. In addition, the Soret effect is added to the simulation. Multicomponent transport is incorporated into the reactor. Since the Aramco model does not include the NO_x component, the GRI 3.0 mech is used to analyze the effect of CO_2 dilution on NO_x formation.

3 Results and discussion

3.1 Experiment and mechanism verification

Figure 4 shows the LBVs comparison between GRI 3.0, Aramco and San Diego mech (Prince et al. 2017) under different equivalence ratios. GRI 3.0 mech and Aramco mech are in good agreement with the measured LBVs of this paper and Refs. (Gu et al. 2000; Bosschaart and Goey, 2004; Halter et al. 2005; Hu et al. 2009a, b; Hermanns et al. 2010; Dirrenberger et al. 2011; Mazas et al. 2011; Goswami et al. 2013; Akram et al. 2013; Li et al. 2015; Nonaka and Pereira 2016; Mitu et al. 2017; Okafor et al. 2018; Han et al. 2019; Wang et al. 2020). The yellow–brown represents lean mixture and light-cyan represents rich mixture. The predictions of San Diego mechanism (Prince et al. 2017) are in good agreement with the experimental results in fuel-lean combustion. However, when equivalence ratio $\Phi \geq 1$, the predictions of LBVs

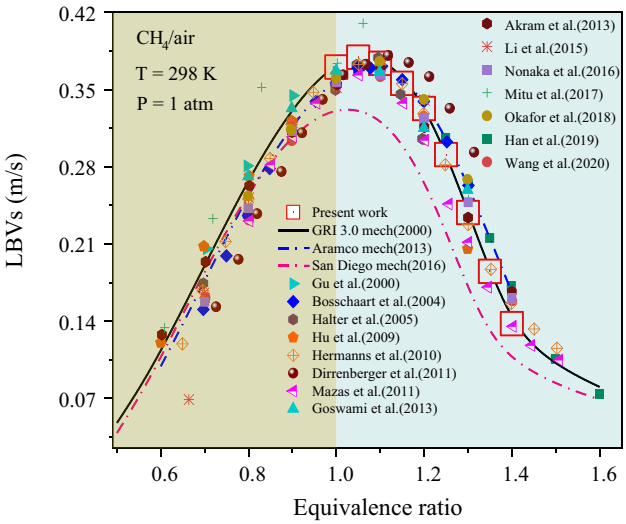

Fig. 4 Laminar burning velocities profile for CH_4/air mixture at 1 atm and 298 K for about 20 years

are lower than the experimental results. Therefore, the San Diego mechanism is not selected for prediction the combustion characteristics of methane in present work.

3.2 Effect of CO_2 addition on laminar burning velocity

In Fig. 5, the solid red line and blue line represent the simulated results of GRI 3.0 and Aramco mech individually. Black dots indicate the LBVs of CH_4 measured experimentally, and gray areas represent the prediction difference between the two mechanisms. From the results of experiments and mechanism predictions, it can be seen that the predicted LBVs of the two mechanisms are not much different when $\Phi \leq 1.15$, and the simulated values of GRI 3.0 mech are slightly larger than that of Aramco mech. However, when the $\Phi \geq 1.15$, the predictions of Aramco mech are higher than that of GRI 3.0 mech. Compared the predicted results of GRI 3.0 and Aramco mech with the experimental measured LBVs, it is found that the gap between experimental results and Aramco mechanism prediction results, and the errors between experiment and simulation are within 5% at same initial condition. This reveals that the process of measuring and calculating LBVs of CH_4 is accurate. As can be seen from Fig. 5, under the same CO_2 doping ratio, the LBVs ascend first and then descend with the increase of equivalence ratio, and when $\Phi = 1.05$, the LBVs reach the maximum. The LBVs became lower linearly as the CO_2 doping ratio increases. This is because the doping ratio of CO_2 increased, reducing the relative percentage of CH_4 in the $CH_4 + CO_2$ mixture. Another reason is that the specific heat capacity of CO_2 is relatively large, which will absorb part of the reaction heat (Burbano

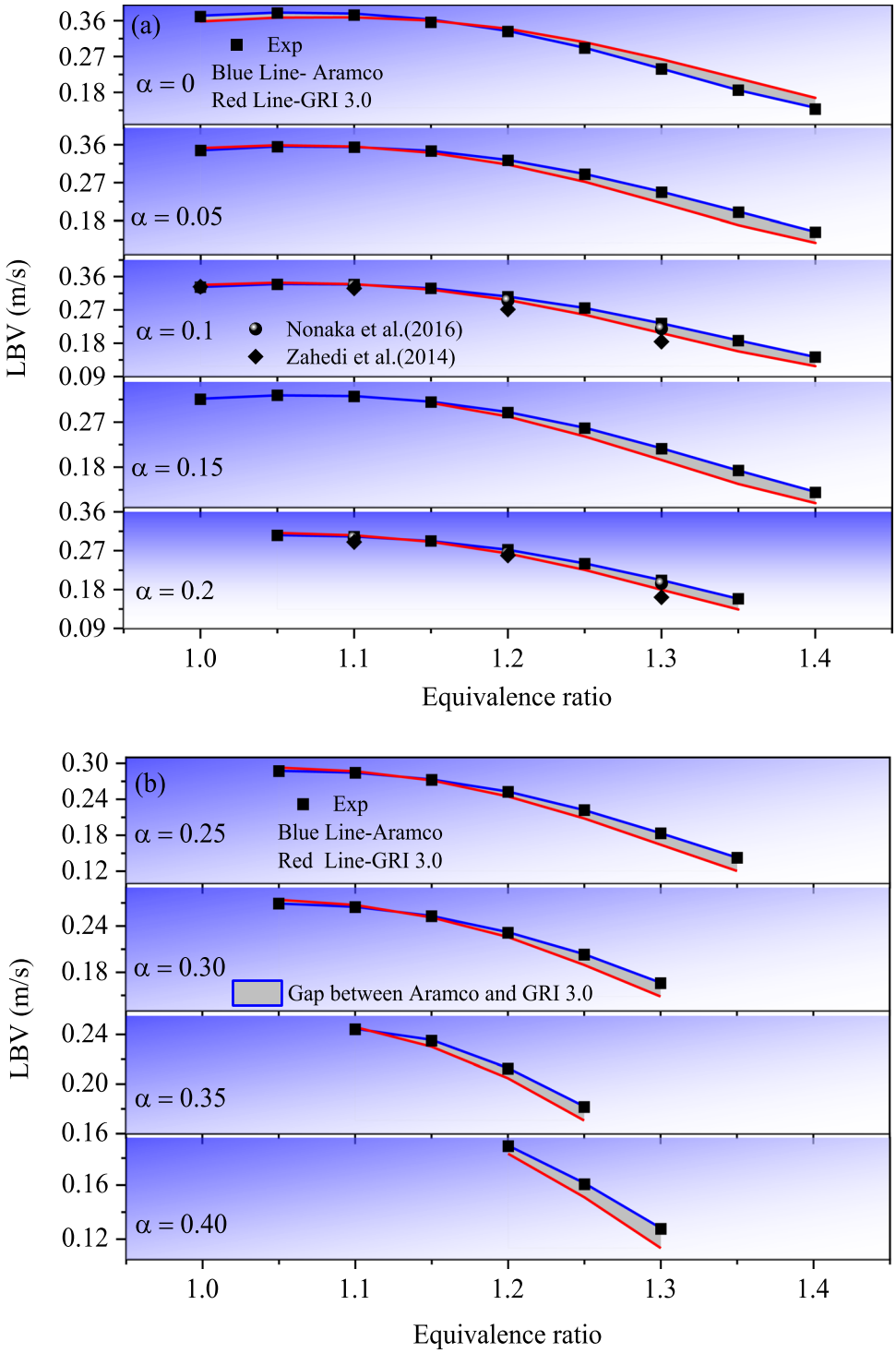

Fig. 5 Comparison of the measured laminar burning velocity with the simulated values

et al. 2011), resulting in the reaction rate and temperature decreased. With the increase of CO_2 doping ratio, the percentage of activated molecules (CH_4+O_2) in reactant decreases, which causes the effective collision times per unit time decrease. Besides, the movement of molecules is decelerated, the number of collisions between reactant molecules per unit time presents a downward trend, and the reaction rate is decelerated. Thus, temperature and LBVs of CH_4 decrease. In addition, the Aramco mechanism simulation results are in good agreement with the other experiments (Nonaka and Pereira 2016; Zahedi and Yousefi 2014).

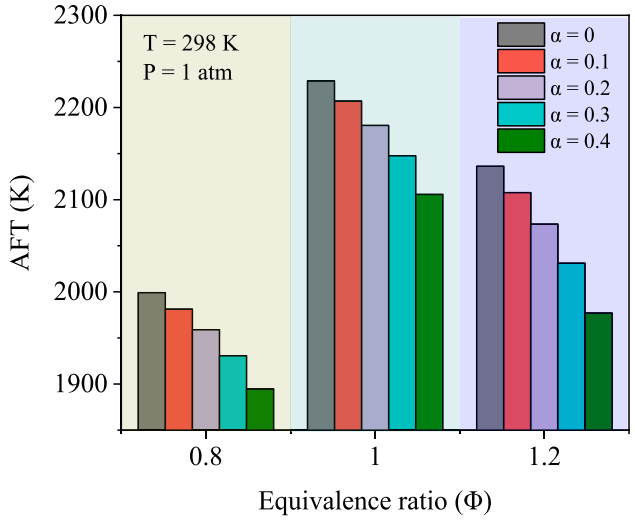

Fig. 6 Peak values of adiabatic flame temperatures change with different CO_2 doping ratios

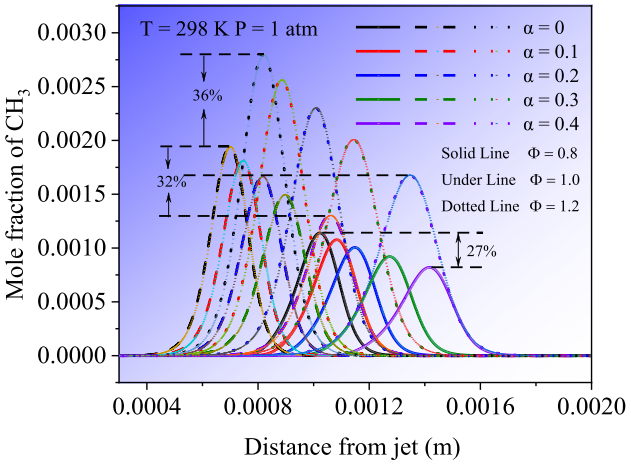

Fig. 7 Intermediate radical CH_3 changes with different CO_2 doping ratios

3.3 Adiabatic flame temperature

Figure 6 shows the effect of CO_2 addition on peak values of AFTs under various equivalence ratios. It can be seen that at the same CO_2 doping ratio, the change trend of AFTs with equivalence ratio is similar to that of LBVs. For example, when CO_2 doping ratio is 0.1, the AFTs are 1981.30 K, 2207.15 K and 2107.74 K at equivalence ratios of 0.8, 1.0 and 1.2, respectively.

At the same CO_2 addition, the AFTs decrease with the increasing of equivalence ratio, and the change trend is the same as that of LBVs. The AFTs are descended with the increase of the CO_2 doping ratio because the content of methane decreases, which leads to lower combustion intensity between fuel and air.

3.4 Intermediates radicals

Combustion is a quite complex process, and a series of intermediates generated in the combustion processing of methane. Based on the above view, Aramco mech was selected for predicting the effect of CO_2 addition on intermediate radicals under different conditions. In order to study the changes of the intermediate radicals with different working conditions, the equivalence ratios of 0.8 (fuel-lean combustion), 1.0 (stoichiometric ratio) and 1.2 (fuel-rich combustion) are chosen for simulation, respectively.

3.4.1 Effect of CO_2 addition on CH_3

Figure 7 shows the change trend of mole fraction of intermediate radical CH_3 with various CO_2 contents under different equivalence ratios. CH_3, as an important intermediate, the maximum mole concentration is reached in the beginning of the reaction, and completely reacts in a relatively short period of time and is no longer generated.

As shown in Fig. 7, firstly, keeping CO_2 doping ratio unchanged, the mole fraction of CH_3 showed a same trend with of the change of equivalence ratio. This is because the proportion of methane gradually increases with the increasing of equivalence ratio. Therefore, CH_3 generated in the oxidation process is gradually increasing. Because the oxidation reaction is the most intense in the slightly fuel-rich combustion ($\Phi = 1.05$), and the AFT is the highest and the LBV is the fastest, the time of CH_3 mole fraction reaching maximum is first advanced and gradually delayed with the increase of the equivalence ratio.

3.4.2 Effect of CO_2 addition on H

Figure 8 shows the effect of CO_2 addition on the H under different equivalence ratios. As the basic intermediate radical, H has an indispensable relationship with LBV and AFT. It reached the maximum mole concentration at beginning of the reaction and existed in the subsequent reaction process.

Compared with CH_3, under the same equivalence ratio and CO_2 doping ratio, the maximum mole fraction of H appeared later than CH_3. This illustrates that the reaction for H formation is later than CH_3. Moreover, the mole fraction of H is much larger than that of CH_3.

As can be seen from Fig. 8, mole fraction of H gradually increases with equivalence ratio becomes larger under the same CO_2 content. The maximum mole fraction shows a trend of advancing first and then postponing from fuel-rich to fuel-lean combustion, which is consistent with that of CH_3. The existence of free radical H lasts longer than CH_3. There maybe two reasons accounting for this. One is that H is decomposed by CH_4 continuously in the oxidation

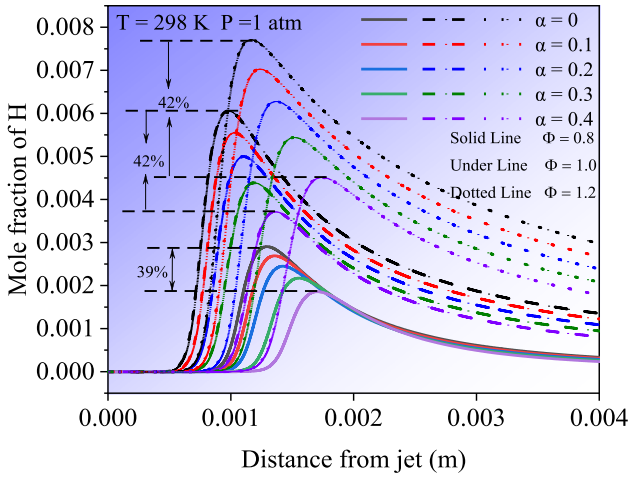

Fig. 8 Intermediate radical H changes with different CO_2 doping ratios

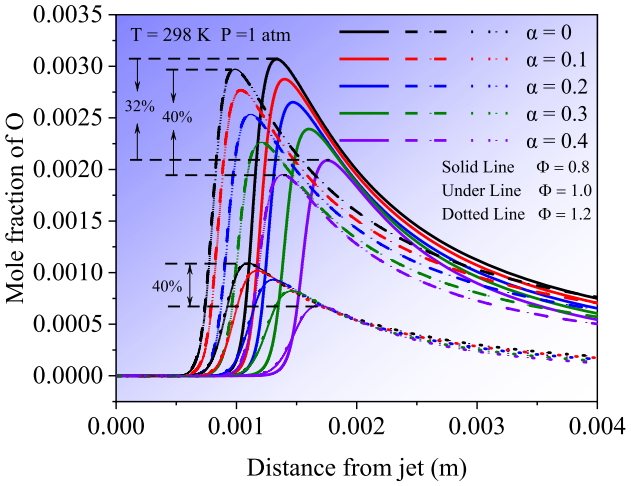

Fig. 10 Intermediate radical O changes with different CO_2 doping ratios

process. The other is that CH_3 also decomposes free radical H in the oxidation process, which makes radical H existed all the time in the whole oxidation process of CH_4.

3.4.3 Effect of CO_2 addition on OH

Figure 9 depicts the intermediate radical OH changes with different CO_2 doping ratios. OH exists all the time in the whole combustion process and gradually decreases, with a smaller decrease than that of H. It is speculated that O_2 continuously participate in the reaction with CH_4 during the combustion process, and oxidative decomposition to generate OH. Under the same CO_2 doping ratio, OH generation time is advanced and then delayed as the equivalence ratio increasing.

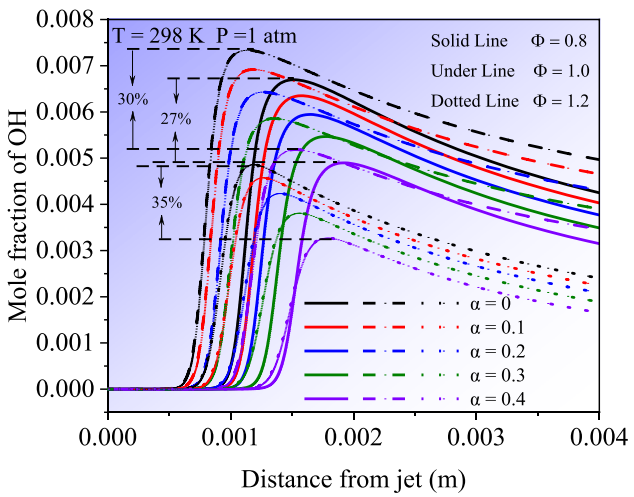

Fig. 9 Intermediate radical OH changes with different CO_2 doping ratios

3.4.4 Effect of CO_2 addition on O

Figure 10 shows the changes of O at different CO_2 doping ratios and equivalence ratios. O as one of important intermediates, the time from the generation to the maximum mole fraction is very short, which is existed in the whole combustion process. From Fig. 10, it can also be found that at the same CO_2 blending ratio, the maximum mole fraction of O drops down slightly with the increasing of equivalence ratio. This is because as the equivalence ratio changes from 0.8 to 1.2, the methane keeps unchanged and the O_2 decreases gradually. Thus, the proportion of O in the combustion process decreases.

3.5 Effect of CO_2 addition on generation of NO_x

NO_x is main pollutant in the process of fuel combustion in internal combustion engine. The majority of nitrogen oxides emitted in combustion are NO, followed by NO_2 and N_2O. NO and NO_2 can be involved in the formation of acid rain and photochemical smog in the atmosphere. N_2O is also a pollutant of interest in recent years, as it is considered a typical greenhouse gas. Therefore, it is great significance to investigate the effect of CO_2 on NO_x formation during methane combustion for high efficiency and low pollution combustion. Because Aramco mech does not contain NO_x, the influence of CO_2 on methane NO_x formation is still predicted by GRI 3.0 mech. Fig. S1 in Supplementary information depicts the NO generation and AFTs of the article by using GRI 3.0 mech compared with the results of other simulation mechanisms. Fig. S2 in Supplementary information shows the NO_x generation of methane mixed with different CO_2 doping ratio when $\Phi = 0.8$, 1.0 and 1.2.

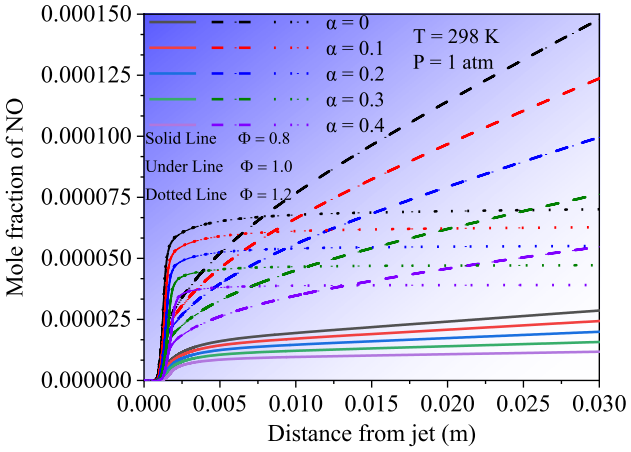

Fig. 11 NO emissions changes with different CO_2 doping ratios

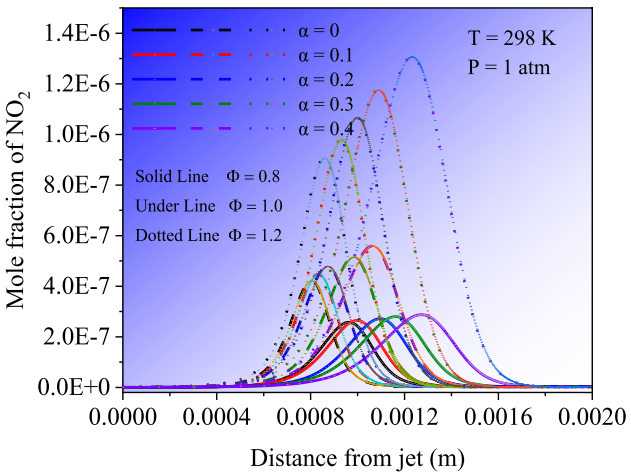

Fig. 12 NO_2 emissions changes with different CO_2 doping ratios

3.5.1 Effect of CO_2 addition on generation of NO

Figure 11 depicts the NO generation under equivalence ratios of 0.8, 1.0 and 1.2 with various CO_2 addition. According to Fig. 11, it can be analyzed that the total NO generation decreases with the increase of CO_2 addition. It is presumed that the generated NO_x is thermal NO_x.

As can be seen from Fig. 11, the equivalence ratio increases from 0.8 to 1.0, and the NO generation amount increases by 5 times. It is speculated that the equivalence ratio increases from 0.8 to 1.0, and the adiabatic flame temperature gradually increases, which results in an increase in thermal NO_x.

3.5.2 Effect of CO_2 addition on generation of NO_2

Figure 12 shows the effect of various CO_2 doping ratio on NO_2 emissions at different equivalence ratios. NO_2, as an intermediate, its variation trend is similar to CH_3, but the difference is that the amount of NO_2 increases monotonously with the increase of the amount of CO_2. Keeping equivalence ratio unchanged, the maximum mole fraction of NO_2 increases and the corresponding time of reaching maximum mole fraction later with the increase of CO_2. When $\Phi = 0.8$, maximum mole fraction of NO_2 and the time of reaching the maximum mole fraction do not change much. The highest concentration and the time of reaching highest concentration is changed obviously while $\Phi = 1.2$.

3.5.3 Effect of CO_2 addition on generation of N_2O

N_2O is a typical greenhouse gas, but the combustion rate can increase by the efficient use of N_2O. Figure 13 depicts the changes of N_2O generation at different equivalence ratios and CO_2 doping ratios. It can be seen that N_2O is an intermediate with a low mole fraction. The generation time and the time of reaching the highest mole fraction is delayed by blending N_2O, and the highest mole fraction increases.

At any equivalence ratio, the maximum N_2O mole fraction has a similar trend with the increase of CO_2 dilution. However, in the subsequent combustion process, the mole fraction decreases as the increasing of blending CO_2.

3.6 Sensitivity analysis

In order to further reveal the impact of blending CO_2 on intermediate radicals and NO_x emissions, the maximum gradient point of temperature is chosen for sensitivity analysis of the effect of CO_2 addition on CH_4 combustion (Dong et al. 2020, 2021). Armaco mech is used to analyze the effect of CO_2 addition on intermediate radicals and GRI 3.0 mech is used to analyze the effect of CO_2 addition on NO_x.

3.6.1 The sensitivity analysis of NO

Figure 14 describes the effect of CO_2 blending on NO production of methane combustion products under different equivalence ratios. The starting path of thermal NO_x is R178 $N + NO = N_2 + O$ and N free radicals are quickly consumed. From the sensitivity analysis of NO_x, it can be seen that the effect on NO production is greater than that of inhibition. R38 $H + O_2 \Leftrightarrow O + OH$ and R240 $CH + N_2 \Leftrightarrow HCN + N$ mainly promote the generation of NO. R35 $H + O_2 + H_2 \Leftrightarrow HO_2 + H_2O$, R125 $CH + O_2 \Leftrightarrow O + HCO$ and R52 $CH_3 + H (+M) \Leftrightarrow CH_4 (+M)$ have strong inhibitory effect on NO production at fuel-lean, stoichiometric ratio and fuel-rich combustion.

For the same elementary reaction, such as R38 $H + O_2 \Leftrightarrow O + OH$, the change trend of sensitivity coefficient is consistent with the equivalence ratio. When $\Phi = 1$, the sensitivity coefficient of R125 $CH + O_2 \Leftrightarrow O + HCO$ decreases with

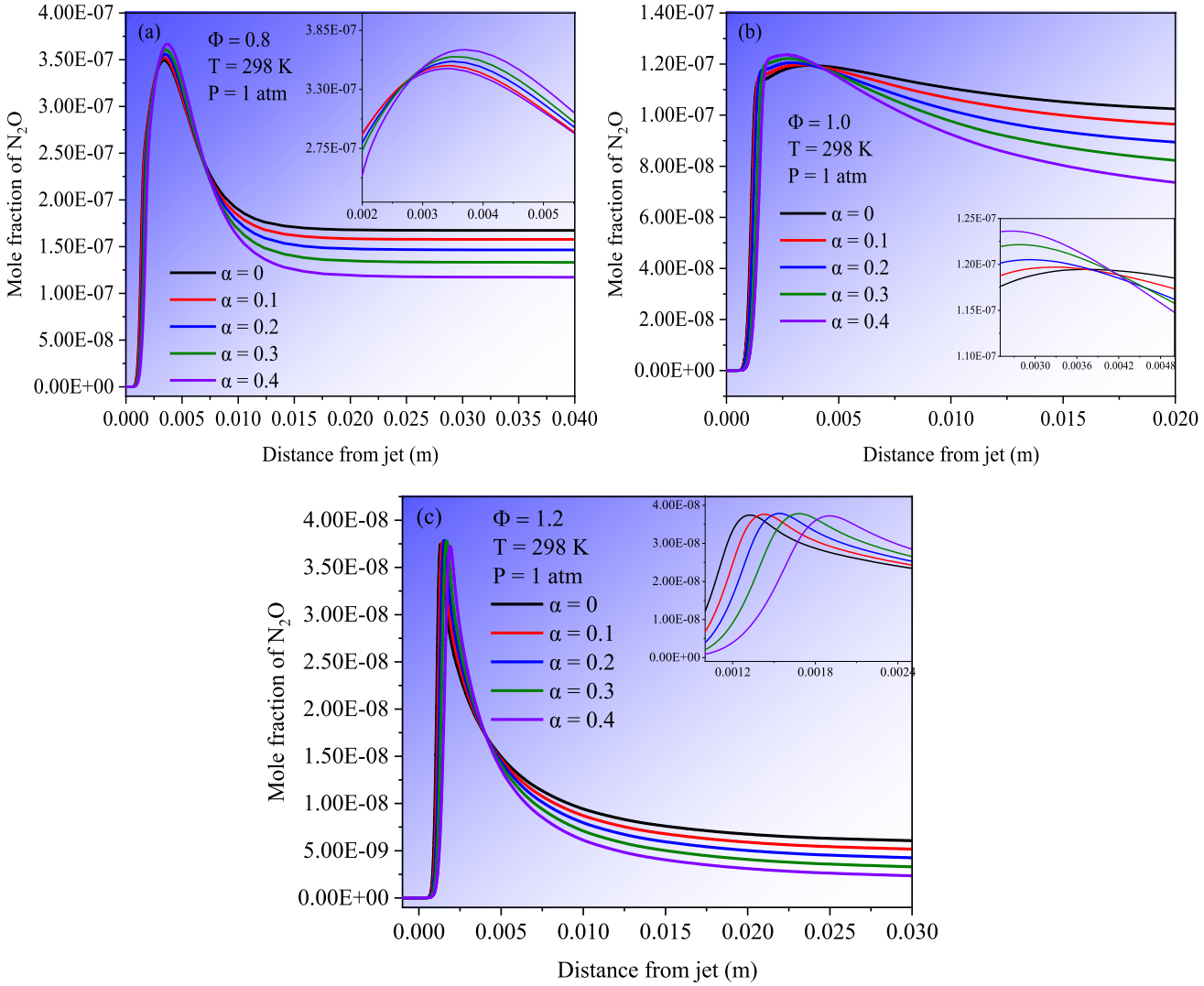

Fig. 13 N_2O emissions changes with different CO_2 doping ratios

the CO_2 doping ratio increases. Different from the change of intermediate radicals, for the same elementary reaction, taking R38 $H+O_2 \Leftrightarrow O+OH$ as an example, the sensitivity coefficient increases continuously with the increase of equivalence ratio, rather than a trend of first increasing and then decreasing.

3.6.2 The sensitivity analysis of NO_2

As can be seen from Fig. 15, different from the effect on NO, R38 $H+O_2 \Leftrightarrow O+OH$ is to inhibit NO_2 generation. R52 $CH_3+H\,(+M) \Leftrightarrow CH_4\,(+M)$ has dominant effect on promoting NO production at all equivalence ratio. In the top 10 elementary reactions, the number of elementary reactions promoting NO_2 generation increases first and then decreases with the increase of equivalence ratio.

At any equivalence ratio, the sensitivity coefficients of R38 $H+O_2 \Leftrightarrow O+OH$ and R52 $CH_3+H(+M) \Leftrightarrow CH_4(+M)$ increases with the increase of CO_2 doping ratio. And the CO_2 addition increases, the increase amplitude is also enhanced.

3.6.3 The sensitivity analysis of N_2O

As can be seen from Fig. 16, R38 $H+O_2 \Leftrightarrow O+OH$ promotes N_2O generation at all equivalence ratios, which is the reaction with the largest sensitivity coefficient among the top 10 elementary reactions. When the Φ is less than or equal to 1.0, R183 $N_2O+H \Leftrightarrow N_2+OH$ mainly inhibits N_2O formation, and the sensitivity coefficient does not change much with the increase of the CO_2 ratio. R52 $CH_3+H(+M) \Leftrightarrow CH_4(+M)$ is inhibited the generation of N_2O at $\Phi=0.8$,

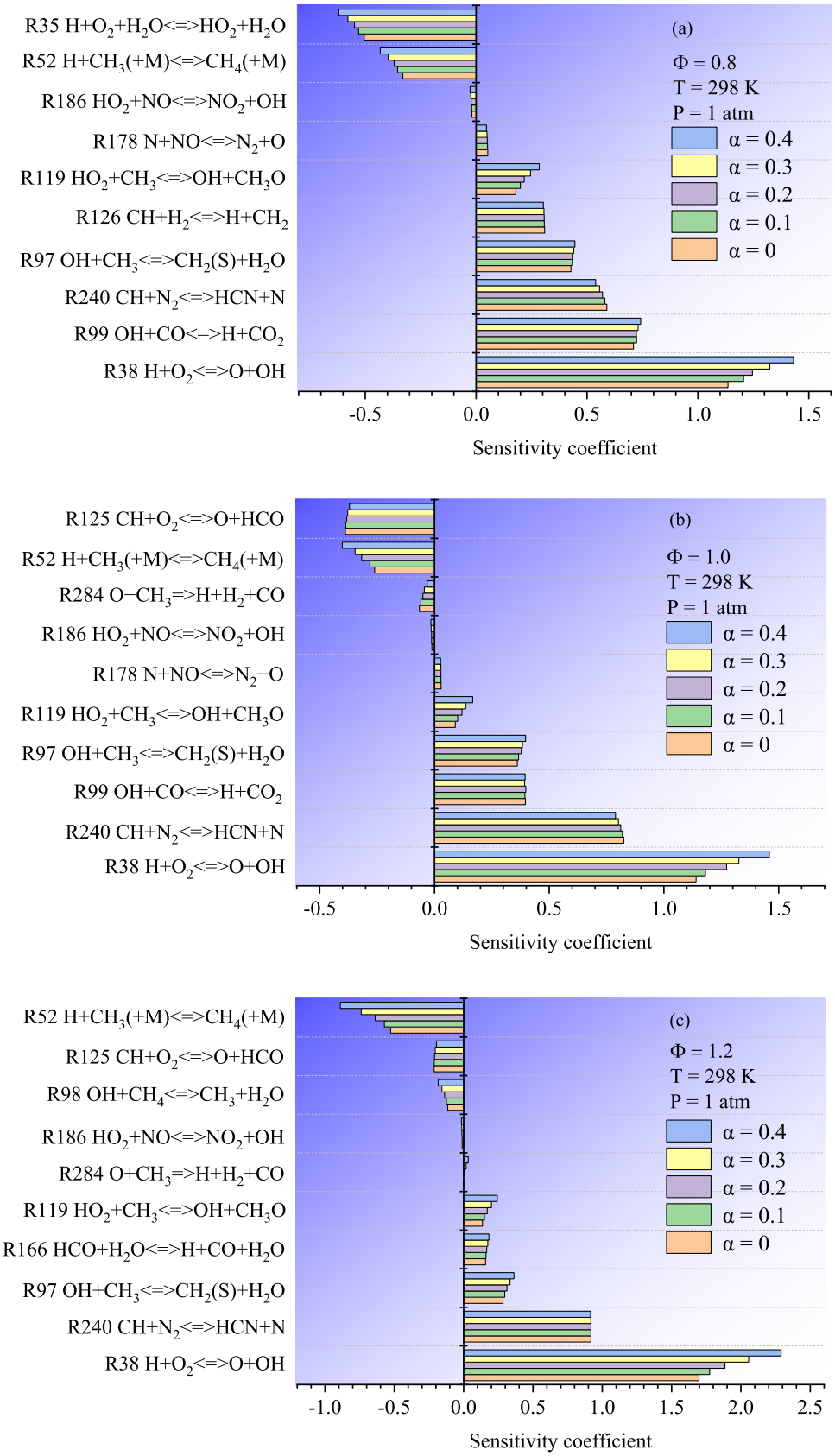

Fig. 14 Sensitivity coefficients with respect to the elementary reactions for NO under different CO_2 doping ratios

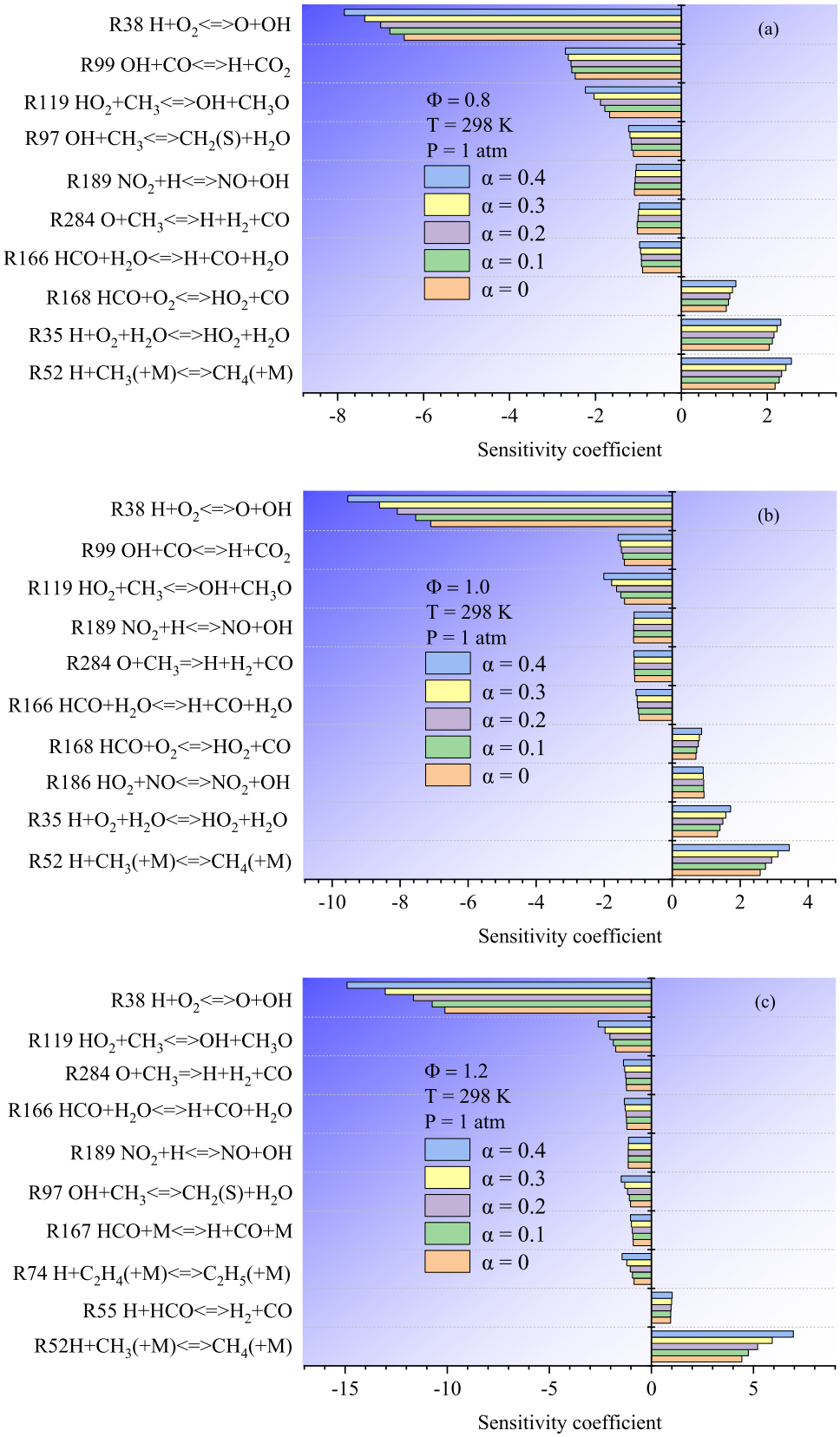

Fig. 15 Sensitivity coefficients with respect to the elementary reactions for NO_2 under different CO_2 doping ratios

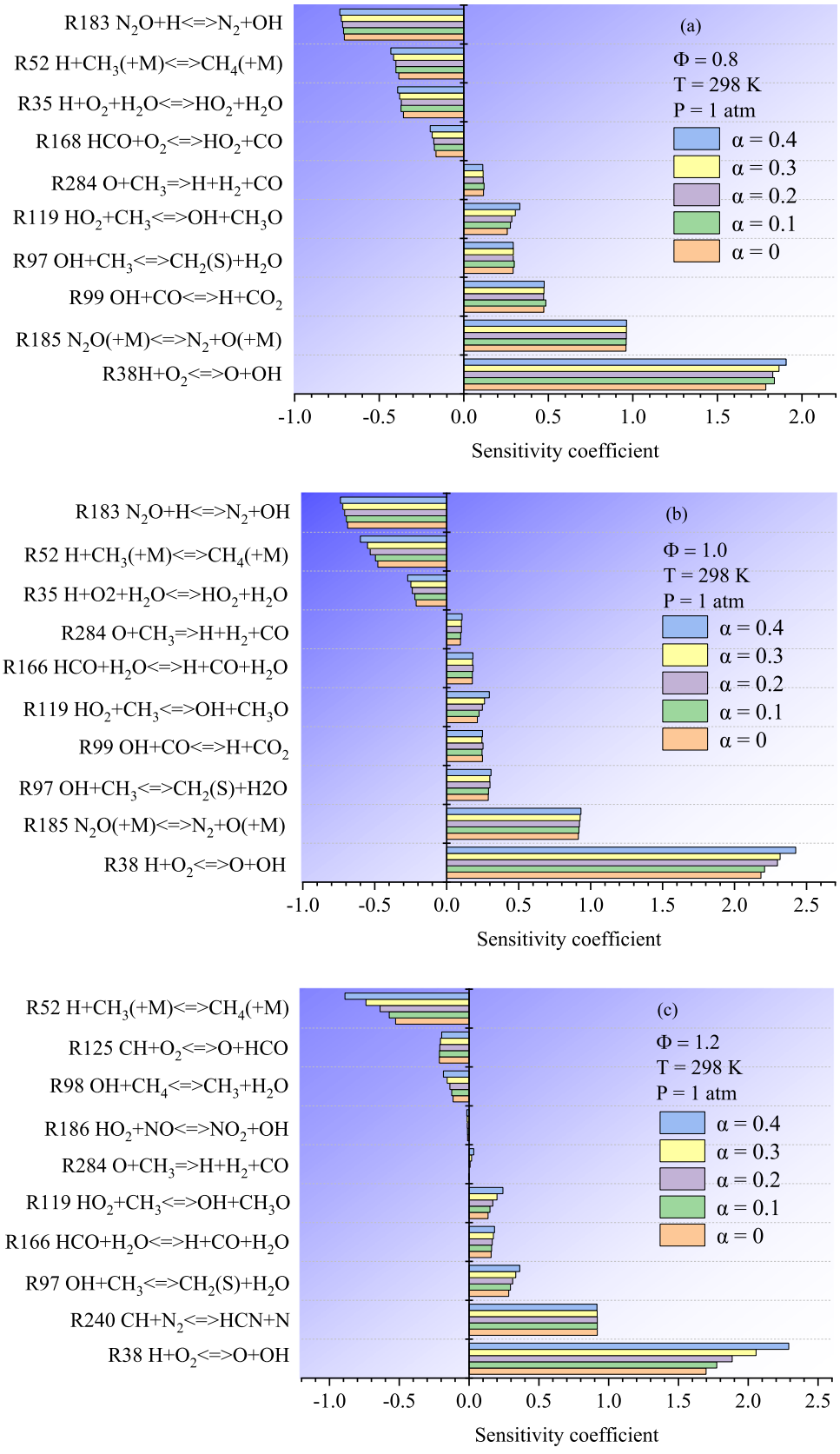

Fig. 16 Sensitivity coefficients with respect to the elementary reactions for N_2O under different CO_2 doping ratios

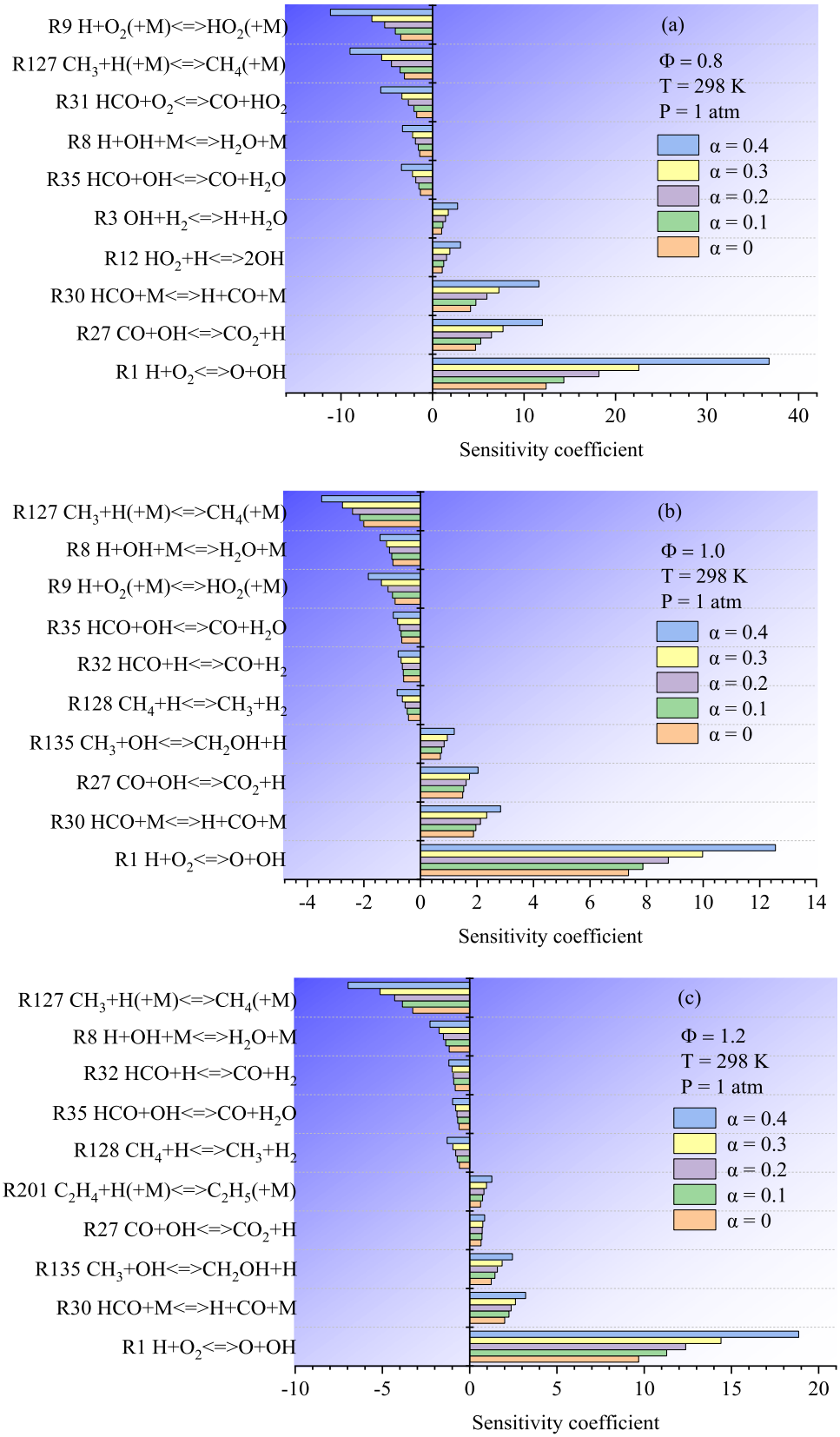

Fig. 17 Sensitivity coefficients with respect to the elementary reactions for CH_3 under different CO_2 doping ratios

1.0 and 1.2, and the sensitivity coefficient increases with increasing CO_2 addition.

3.6.4 The sensitivity analysis of CH_3, H, OH and O

According to the results, when the CO_2 doping ratio stays unchanged, the sensitivity coefficient decreases first and then increases as the increasing of equivalence ratio. In the top 10 reactions that have a great influence on formation of CH_3, the sensitivity coefficient of reactions that promote the generation of CH_3 with the increase of the equivalence ratio decreases and then increases. The change trend is opposite to that of LBVs, AFTs, intermediate radicals.

At the same equivalence ratio, it can be seen in Fig. 17 that the CH_3 sensitivity coefficient increases with the increase of the CO_2 addition, and the increase in sensitivity coefficient becomes larger with the increase of CO_2 addition. This is because with the increasing of CO_2 addition, the decrease in AFT gradually increasing and the sensitivity coefficient becomes larger, which means the reactions become more sensitive with temperature change. The generation of CH_3 is promoted by R1 $H+O_2 \Leftrightarrow O+OH$. When $\Phi=0.8$, R9 $H+O_2(+M) \Leftrightarrow HO_2(+M)$ plays the main role of inhibition. When Φ is greater than or equal to 1, R127 $CH_3+H(+M) \Leftrightarrow CH_4(+M)$ has a negative effect on generation of CH_3.

Figures S3–S5 in Supplementary information report the H, OH and O sensitivity coefficients with respect to the elementary reactions, respectively.

4 Conclusions

In this paper, CO_2 is used as an additive to study its blending on the methane laminar combustion characteristics and the NO_x emission characteristics. The study starts from studying the effect of blending a wide range of CO_2 concentrations on the methane combustion characteristics through a combination of experiments and numerical simulations. The second mission is to analyze the effect of CO_2 on NO_x production during methane combustion from the molar amount of NO_x to the temperature sensitivity of NO_x. The reliability of the simulation results is verified by comparing the laminar burning velocity measured by Bunsen burner with CHEMKIN simulations, with the main parameter being the laminar combustion velocity. With the increase of equivalence ratio, laminar burning velocity increases first and then decreases. The laminar burning velocity reaches the maximum when the equivalence ratio is 1.05. GRI 3.0 mech and experimental results have good agreement in measuring the laminar burning velocity of pure CH_4, but after blending CO_2, the laminar burning velocity predicted by the Aramco mechanism is highly fitted to the experimental results. The predictions of the two mechanisms are different. When Φ is less than or equal to 1.15, the prediction of GRI 3.0 mech is greater than that of Aramco mech, but when $\Phi>1.15$, the predicted result by Aramco mech is greater than the simulated value of GRI 3.0 mech. At any equivalence ratio, the laminar burning velocity of CH_4 decreases with the increase of CO_2 addition. Blending carbon dioxide absorbs the heat of reaction in the combustion process, resulting in a decrease in the adiabatic flame temperature. Aramco mech is selected to analyze the effect of CO_2 addition to the adiabatic flame temperature, intermediate radicals, and the sensitivity analysis of the intermediate radicals, it was found that adiabatic flame temperature and the maximum mole fraction of the intermediate radicals decreases after blending CO_2. Through sensitivity analysis, it is found that the elementary reaction $H+O_2 \Leftrightarrow O+OH$ always promotes the generation of free radicals, and the sensitivity coefficient of the elementary reaction gradually decreases with the increase of CO_2 doping ratio. The effect of CO_2 on the NO_x emissions (NO, NO_2 and N_2O), and sensitivity analysis of NO_x formation is predicted by GRI 3.0 mech. The results of numerical simulation show that the amount of NO_x generates or the maximum mole fraction point decreases by blending CO_2. The elementary reaction $H+O_2 \Leftrightarrow O+OH$ also always promotes NO_x emission. The results of this study show the effect of CO_2 on methane combustion characteristics and NO_x emission, which provides insight for further effective utilization of CO_2. However, subsequent studies can be conducted by only verifying the effect of CO_2 on methane, and subsequent studies should be conducted for the blending of CO_2 with macromolecular hydrocarbon fuels and oxygenated fuels.

Supplementary Information The online version contains supplementary material available at https://doi.org/10.1007/s40789-023-00655-9.

Acknowledgements The authors would like to thank the National Natural Science Foundation of China (52176095), Anhui Provincial Natural Science Foundation (2008085J25), and the Project of support program for outstanding young people in Colleges and Universities (gxyqZD201830) for their financial support of this study.

Author contribution WD: Software, Data curation, Writing—review & editing. LX: Data curation, Writing—original draft. JG: Data curation, Writing—review & editing. BQ: Data curation, Writing—review & editing. HC: Resources, Funding acquisition, Project administration, Writing—review & editing.

Declarations

Competing interest The authors declare that they have no conflict of interests regarding the publication of this paper.

References

Akram M, Saxena P, Kumar S (2013) Laminar burning velocity of methane-air mixtures at elevated temperatures. Energy Fuels 27:3460–3466. https://doi.org/10.1021/ef4009218

Ao CC, Feng BB, Qian SY, Wang L, Zhao W, Zhai YT, Zhang LD (2020) Theoretical study of transition metals supported on g-C_3N_4 as electrochemical catalysts for CO_2 reduction to CH_3OH and CH_4. J CO_2 Util 36:116–123. https://doi.org/10.1016/j.jcou.2019.11.007

Azatyan VV, Shebeko YN, Shebeko AY (2010) A numerical modelling of an influence of CH_4, N_2, CO_2 and steam on a laminar burning velocity of hydrogen in air. J Loss Prevent Proc 23:331–336. https://doi.org/10.1016/j.jlp.2009.12.002

Bosschaart KJ, de Goey LPH (2004) The laminar burning velocity of flames propagating in mixtures of hydrocarbons and air measured with the heat flux method. Combust Flame 136:261–269. https://doi.org/10.1016/j.combustflame.2003.10.005

Burbano HJ, Pareja J, Amell AA (2011) Laminar burning velocities and flame stability analysis of H_2/CO/air mixtures with dilution of N_2 and CO_2. Int J Hydrog Energy 36:3232–3242. https://doi.org/10.1016/j.ijhydene.2010.11.089

Chu HQ, Ren F, Xiang LK, Dong SL, Qiao F, Xu GJ (2019) Numerical investigation on combustion characteristics of laminar premixed n-heptane/air flames at elevated initial temperature and pressure. J Energ Inst 92:1821–1830. https://doi.org/10.1016/j.joei.2018.11.010

Chu H, Xiang L, Nie X, Ya Y, Gu M, E JQ (2020) Laminar burning velocity and pollutant emissions of the gasoline components and its surrogate fuels: a review. Fuel 269:117451. https://doi.org/10.1016/j.fuel.2020.117451

Chu HQ, Xiang LK, Meng S, Dong WL, Gu MY, Li ZH (2021) Effects of N_2 dilution on laminar burning velocity, combustion characteristics and NO_x emissions of rich CH_4-air premixed flames. Fuel 284:119017. https://doi.org/10.1016/j.fuel.2020.119017

Dirrenberger P, Le Gall H, Bounaceur R, Herbinet O, Glaude PA, Konnov A, Battin-Leclerc F (2011) Measurements of laminar flame velocity for components of natural gas. Energy Fuels 25:3875–3884. https://doi.org/10.1021/ef200707h

Dong WL, Hu JL, Xiang LK, Chu HQ, Li ZH (2020) Numerical investigation on combustion characteristics of laminar premixed n-heptane/hydrogen/air flames at elevated pressure. Energy Fuels 34:14768–14775. https://doi.org/10.1021/acs.energyfuels.0c02318

Dong WL, Jin T, Qiu BB, Chu HQ (2021) Effects of carbon dioxide on the combustion characteristics of the laminar premixed n-heptane/air flames at elevated pressures. J Energy Inst 99:127–136. https://doi.org/10.1016/j.joei.2021.08.011

Ghabi A, Boushaki T, Bocanegra PE, Robert E (2023) Laminar burning velocity, adiabatic flame temperature, and pollutants of biogas/air mixture at various CO_2 concentrations and plasma assist. Combust Sci Technol 195:1599–1621. https://doi.org/10.1080/00102202.2023.2182202

Goswami M, Derks SCR, Coumans K, Slikker WJ, de Andrade Oliveira MH, Bastiaans R, Luijten CCM, de Goey LPH, Konnov AA (2013) The effect of elevated pressures on the laminar burning velocity of methane+air mixtures. Combust Flame 160:1627–1635. https://doi.org/10.1016/j.combustflame.2013.03.032

Gu XJ, Haq MZ, Lawes M, Wooley R (2000) Laminar burning velocity and Markstein lengths of methane-air mixtures. Combust Flame 121:41–58. https://doi.org/10.1016/S0010-2180(99)00142-X

Guo HW, Chen MQ, Zhong Q, Wang YN, Ma WH, Ding J (2019) Synthesis of Z-scheme α-Fe_2O_3/g-C_3N_4 composite with enhanced visible-light photocatalytic reduction of CO_2 to CH_3OH. J CO_2 Util 33:233–241. https://doi.org/10.1016/j.jcou.2019.05.016

Halter F, Chauveau C, Djebaïli-Chaumeix N, Gökalp I (2005) Characterization of the effects of pressure and hydrogen concentration on laminar burning velocities of methane–hydrogen–air mixtures. Proc Combust Inst 30:201–208. https://doi.org/10.1016/j.proci.2004.08.195

Han XL, Wang ZH, He Y, Wang SX, Zhu YQ, Konnov AA (2019) Over-rich combustion of CH_4, C_2H_6, and C_3H_8+air premixed flames investigated by the heat flux method and kinetic modeling. Combust Flame 210:339–349. https://doi.org/10.1016/j.combustflame.2019.09.009

Hermanns RTE, Konnov AA, Bastiaans RJM, Goey LPH, Lucka K, Köhne H (2010) Effects of temperature and composition on the laminar burning velocity of CH_4+H_2+O_2+N_2 flames. Fuel 89:114–121. https://doi.org/10.1016/j.fuel.2009.08.010

Hu EJ, Huang ZH, Zheng JQ, Li QQ, He JJ (2009a) Numerical study on laminar burning velocity and NO formation of premixed methane-hydrogen-air flames. Int J Hydrog Energy 34:6545–6557. https://doi.org/10.1016/j.ijhydene.2009.05.080

Hu EJ, Huang ZH, He JJ, Jin C, Zhang JJ (2009b) Experimental and numerical study on laminar burning characteristics of premixed methane-hydrogen-air flames. Int J Hydrog Energy 34(11):4876–4888. https://doi.org/10.1016/j.ijhydene.2009.03.058

Huang QW, Luo QM, Wang YF, Pentzer E, Gurkan B (2019) Hybrid ionic liquid capsules for rapid CO_2 capture. Ind Eng Chem Res 58:10503–10509. https://doi.org/10.1021/acs.iecr.9b00314

Jithin EV, Varghese RJ, Velamati RK (2020) Experimental and numerical investigation on the effect of hydrogen addition and N_2/CO_2 dilution on laminar burning velocity of methane/oxygen mixtures. Int J Hydrog Energy 45:16838–16850. https://doi.org/10.1016/j.ijhydene.2020.04.105

Li XC, Fang ZM (2014) Current status and technical challenges of CO_2 storage in coal seams and enhanced coalbed methane recovery: an overview. Ins J Coal Sci Technol 1:93–102. https://doi.org/10.1007/s40789-014-0002-9

Li GS, Liang JJ, Zhang ZH, Tian L, Cai Y, Tian LY (2015) Experimental investigation on laminar burning velocities and Markstein lengths of premixed methane-n-heptane-air mixtures. Energy Fuels 29:4549–4556. https://doi.org/10.1021/acs.energyfuels.5b00355

Liu G, Zhou J, Wang Z, Yang W, Liu J, Cen K (2020) Adiabatic laminar burning velocities of C_3H_8–O_2–CO_2 and C_3H_8–O_2–N_2 mixtures at ambient conditions-part II: mechanistic interpretation. Fuel 276:117946. https://doi.org/10.1016/j.fuel.2020.117946

Ma DS, Sun ZY (2020) The progress on the studies about NO_x emission in PFI-H_2ICE. Int J Hydrog Energy 45:10580–10591. https://doi.org/10.1016/j.ijhydene.2019.11.065

Mazas AN, Fiorina B, Lacoste DA, Schuller T (2011) Effects of water vapor addition on the laminar burning velocity of oxygen-enriched methane flames. Combust Flame 158:2428–2440. https://doi.org/10.1016/j.combustflame.2011.05.014

Metcalfe WK, Burke SM, Ahmed SS, Curran HJ (2013) A hierarchical and comparative kinetic modeling study of C_1–C_2 hydrocarbon and oxygenated fuels. Int J Chem Kinet 45:638–675. https://doi.org/10.1002/kin.20802

Mitu M, Giurcan V, Razus D, Oancea D (2017) Inert gas influence on the laminar burning velocity of methane-air mixtures. J Hazard Mater 321:440–448. https://doi.org/10.1016/j.jhazmat.2016.09.033

Moffat RJ (1988) Describing the uncertainties in experimental results. Exp Therm Fluid Sci 1:3–17. https://doi.org/10.1016/0894-1777(88)90043-X

Movileanu C, Razus D, Oancea D (2011) Additive effects on the burning velocity of ethylene–air mixtures. Energy Fuels 25(6):2444–2451. https://doi.org/10.1021/ef200183h

Nonaka HOB, Pereira FM (2016) Experimental and numerical study of CO_2 content effects on the laminar burning velocity of biogas. Fuel 182:382–390. https://doi.org/10.1016/j.fuel.2016.05.098

Okafor EC, Naito Y, Colson S, Ichikawa A, Kudo T, Hayakawa A, Kobayashi H (2018) Experimental and numerical study of the laminar burning velocity of CH_4–NH_3–air premixed flames. Combust Flame 187:185–198. https://doi.org/10.1016/j.combustflame.2017.09.002

Prince JC, Treviño C, Williams FA (2017) A reduced reaction mechanism for the combustion of n-butane. Combust Flame 175:27–33. https://doi.org/10.1016/j.combustflame.2016.06.033

Razus D, Oancea D, Brinzea V, Mitu M, Movileanu C (2010) Experimental and computed burning velocities of propane-air mixtures. Energy Convers Manag 51:2979–2984. https://doi.org/10.1016/j.enconman.2010.06.041

Ren F, Chu HQ, Xiang LK, Han WW, Gu MY (2019a) Effect of hydrogen addition on the laminar premixed combustion characteristics. J Energ Inst 92:1178–1190. https://doi.org/10.1016/j.joei.2018.05.011

Ren F, Xiang LK, Chu HQ, Jiang HT, Ya YC (2019b) Modeling study of the impact of blending N_2, CO_2, and H_2O on characteristics of CH_4 laminar premixed combustion. Energy Fuels 34:1184–1192. https://doi.org/10.1021/acs.energyfuels.9b02108

Ren F, Xiang LK, Chu HQ, Ya YC, Han WW, Nie XK (2020) Numerical investigation on theeffect of CO_2 and Steam for the H_2 intermediate formation and NO_x emission in laminarpremixed methane/sir flames. Int J Hydrog Energy 45:3785–3794. https://doi.org/10.1016/j.ijhydene.2019.05.096

Sampath S, Jithin EV, Kumbhakarna N, Kumar S (2023) Experimental investigations on laminar burning velocity variation of CH_4+air mixtures at elevated temperatures with CO_2 and N_2 dilution. J Therm Anal Calorim 148:2517–2526. https://doi.org/10.1007/s10973-022-11917-0

Shamiri A, Shafeeyan MS, Tee HC, Leo CY, Aroua MK, Aghamohammadi N (2016) Absorption of CO_2 into aqueous mixtures of glycerol and monoethanolamine. J Nat Gas Sci Eng 35:605–613. https://doi.org/10.1016/j.jngse.2016.08.072

Shang RX, Zhuang ZX, Yang Y, Li G (2022) Laminar flame speed of H_2/CH_4/air mixtures with CO_2 and N_2 dilution. Int J Hydrog Energy 47:32315–32329. https://doi.org/10.1016/j.ijhydene.2022.07.099

Smith G, Golden D, Frenklach M (2000) GRI 3.0[EB/OL]. Gas Research Institute, Chicago, IL. Available at http://www.me.berkeley.edu/gri_mech/

Sun ZY, Xu CS (2020) Turbulent burning velocity of stoichiometric syngas flames with different hydrogen volumetric fractions upon constant-volume method with multi-zone model. Int J Hydrog Energy 45:4969–4978. https://doi.org/10.1016/j.ijhydene.2019.12.054

Talapaneni SN, Singh G, Kim IY, AlBahily K, Al-Muhtaseb AH, Karakoti AS, Tavakkoli E, Vinu A (2019) Nanostructured carbon nitrides for CO_2 capture and conversion. Adv Mater. https://doi.org/10.1002/adma.201904635

Ueda A, Nisida K, Matsumura Y, Ichikawa T, Nakashimada Y, Endo T, Kim W (2021) Effects of hydrogen and carbon dioxide on the laminar burning velocities of methane–air mixtures. J Energy Inst 99:178–185. https://doi.org/10.1016/j.joei.2021.09.007

Wang JH, Huang ZH, Kobayashi H, Ogami Y (2012) Laminar burning velocities and flame characteristics of CO–H_2–CO_2–O_2 mixtures. Int J Hydrog Energy 37:19158–19167. https://doi.org/10.1016/j.ijhydene.2012.07.103

Wang ZH, Weng WB, He Y, Li ZS, Cen KF (2015) Effect of H_2/CO ratio and N_2/CO_2 dilution rate on laminar burning velocity of syngas investigated by direct measurement and simulation. Fuel 141:285–292. https://doi.org/10.1016/j.fuel.2014.10.040

Wang SX, Wang ZH, He Y, Han XL, Sun ZW, Zhu YQ, Costa M (2020) Laminar burning velocities of CH_4/O_2/N_2 and oxygen-enriched CH_4/O_2/CO_2 flames at elevated pressures measured using the heat flux method. Fuel 259:116152. https://doi.org/10.1016/j.fuel.2019.116152

Wang HL, Lei QL, Li PP, Liu CL, Xue YP, Zhang XW, Li CF, Yang ZB (2021) Key CO_2 capture technology of pure oxygen exhaust gas combustion for syngas-fueled high-temperature fuel cells. Ins J Coal Sci Technol 8:383–393. https://doi.org/10.1007/s40789-021-00445-1

Wang N, Dong X, Liu Y, Zhang SF, Wu H, Hernndez JJ (2022) Effects of CO_2 on the laminar burning velocities of toluene reference fuel (TRF) with increasing initial temperatures and pressures. Fuel 318:123508. https://doi.org/10.1016/j.fuel.2022.123508

Xiang LK, Chu HQ, Ren F, Gu MY (2019) Numerical analysis of the effect of CO_2 on combustion characteristics of laminar premixed methane/air flames. J Energy Inst 92:1487–1501. https://doi.org/10.1016/j.joei.2018.06.018

Xiang LK, Jiang HT, Ren F, Chu HQ, Wang P (2020) Numerical study of the physical and chemical effects of hydrogen addition on laminar premixed combustion characteristics of methane and ethane. Int J Hydrog Energy 45:20501–20514. https://doi.org/10.1016/j.ijhydene.2019.11.040

Zahedi P, Yousefi K (2014) Effects of pressure and carbon dioxide, hydrogen and nitrogen concentration on laminar burning velocities and NO formation of methane-air mixtures. J Mech Sci Technol 28:377–386. https://doi.org/10.1007/s12206-013-0970-5

Zhang B, Dong C, Zhou Q, Chen X, Culligan PJ, Zhao Q, Xu T, Hui S (2015) Experimental study on laminar flame speed of natural gas/carbon monoxide/air mixtures. Energy Sour Part A 37:576–582. https://doi.org/10.1080/15567036.2011.588681

Zhang XC, Zhang ZJ, Li X, Chen YF, Wang XH (2021) Study on stretch extinction characteristics of methane/carbon dioxide versus oxygen/carbon dioxide counterflow non-premixed combustion under elevated pressures. J Nat Gas Sci Eng 92:103994. https://doi.org/10.1016/j.jngse.2021.103994